Design and Development of an SAE Micro Class Aircraft

Team Number: 319

"Flying Anvils"

University of Minnesota - Twin Cities

Team Members:

Tyler Coffey
Steve Eyberg
Sean Gamlin
Adem Rudin*
Nick Simon
Andrew Swift
David Towey
Brandon Wiegert

SAE®

Appendix
2009 SAE AERO DESIGN

STATEMENT OF COMPLIANCE
Certification of Qualification

Team Name: Flying Anvils   Team Number: 319

School: University of Minnesota

Faculty Advisor: Jeff Hammer

Faculty Advisor E-Mail: hammer@aem.umn.edu

Statement of Compliance

As Faculty Advisor, I certify that the registered team members are enrolled in collegiate courses. This team has designed, constructed and/or modified the radio controlled airplane they will use for the SAE Aero Design 2009 competition, without direct assistance from professional engineers, R/C model experts or pilots, or related professionals.

Signature of Faculty Advisor

Team Captain Information:

Team Captain:	Adem Rudin
Captain's E-mail:	rudi0026@umn.edu
Captain's Phone:	612-360-7274

Note: A copy of this statement needs to be included in your Design Report as page 2 (see 60.1).

Contents

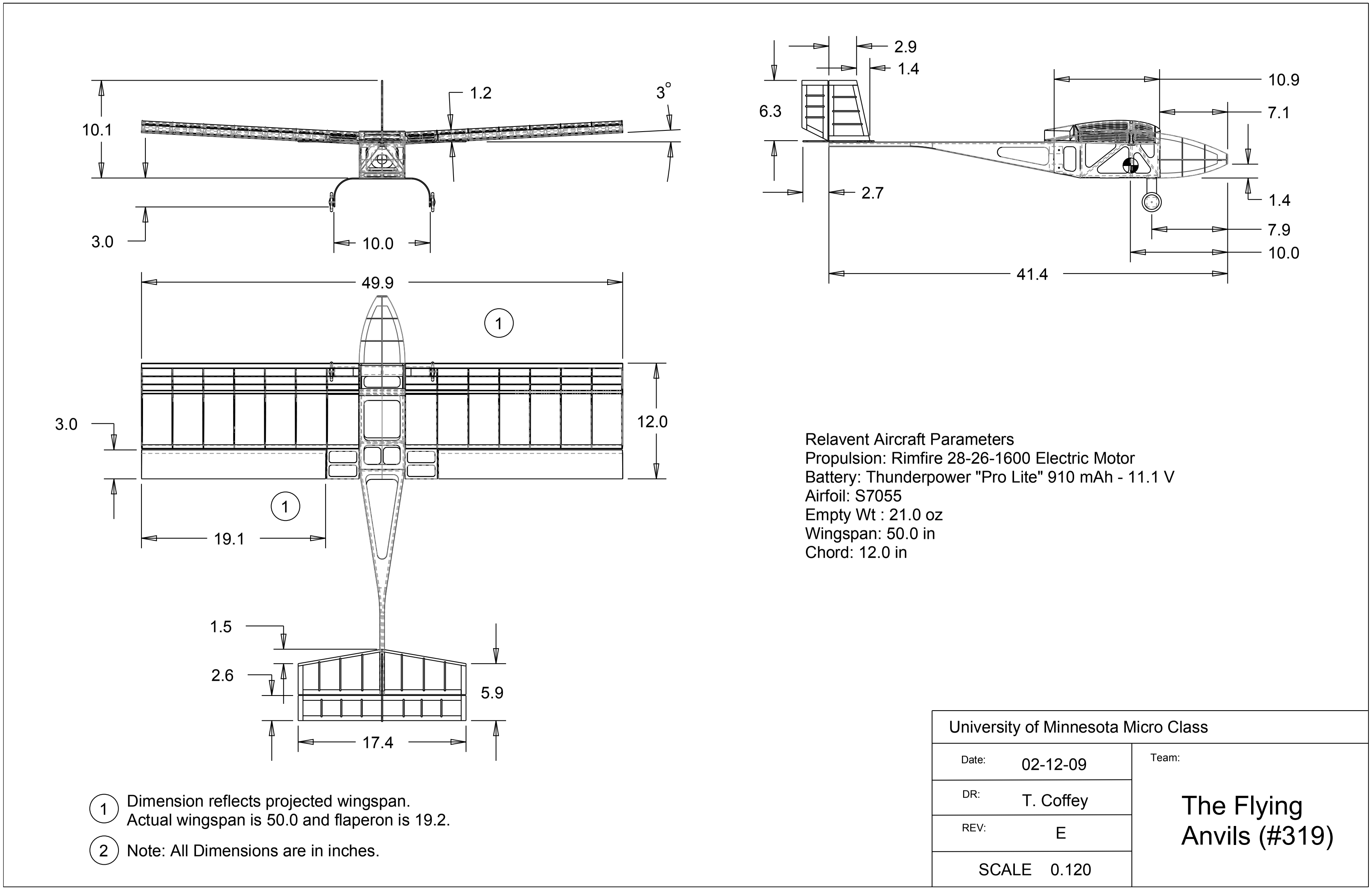
10.1
1.2
3°
3.0
10.0
49.9
1
3.0
12.0
1
19.1
1.5
2.6
5.9
17.4
2.9
1.4
6.3
10.9
7.1
2.7
1.4
7.9
10.0
41.4
Relavent Aircraft Parameters
Propulsion: Rimfire 28-26-1600 Electric Motor
Battery: Thunderpower "Pro Lite" 910 mAh - 11.1 V
Airfoil: S7055
Empty Wt : 21.0 oz
Wingspan: 50.0 in
Chord: 12.0 in
1 Dimension reflects projected wingspan.
Actual wingspan is 50.0 and flaperon is 19.2.
2 Note: All Dimensions are in inches.
University of Minnesota Micro Class
Date: 02-12-09
DR: T. Coffey
REV: E
SCALE 0.120
Team:
The Flying
Anvils (#319)

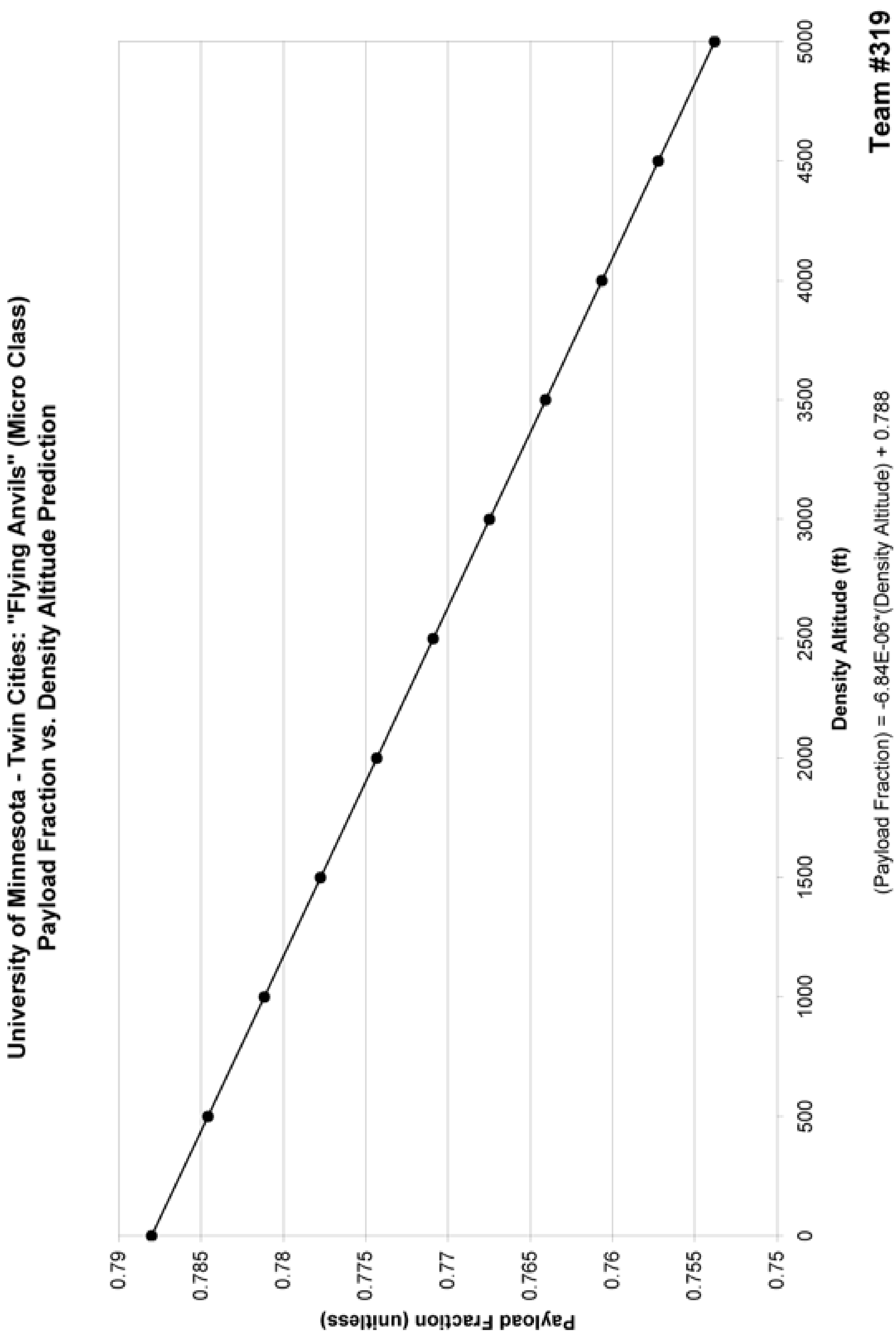
University of Minnesota - Twin Cities: "Flying Anvils" (Micro Class)
Payload Fraction vs. Density Altitude Prediction
Payload Fraction (unitless)
0.79
0.785
0.78
0.775
0.77
0.765
0.76
0.755
0.75
0
500
1000
1500
2000
2500
3000
3500
4000
4500
5000
Density Altitude (ft)
(Payload Fraction) = -6.84E-06*(Density Altitude) + 0.788
Team #319

INTRODUCTION

SAE holds twelve different collegiate design competitions annually. One of the competitions is the Aero Design Challenge, a competition to design, build, and test the performance of an air scale vehicle. The competition is divided into three divisions: Micro, Regular, and Open Class. Micro Class has more challenges pertaining to the weight and size constraints of the aircraft; Regular Class is the entry-level competition; and Open Class is more difficult due to little limitations on the design parameters and the requirement to take off from a non-developed airstrip.

UAV's are of high interest to many people in many applications. The military is the number one source that desires the development of micro UAV's and technology has made this possible. The Micro Class competition requires aircraft that are portable, have a payload area that could hold a video or still camera, and be quick and easy to assemble by a team of two people.

This team's objective was to design and build a highly competitive Micro Class aircraft for entry in to the SAE Aero Design Challenge. We believe we have achieved this by extensive research in to the methods of remote-control aircraft design, construction, and operation; detailed in the following report.

REQUIREMENTS

The Micro Class division of the SAE Aero Design competition requires participants to engineer a small remote-controlled aircraft that is easily disassembled, and is capable of carrying a payload. The scoring equation drives teams to create an aircraft that can carry the a large payload, while keeping its empty weight to a minimum. The aircraft must contain a payload compartment that fits an 8 in $\times$ 4 in $\times$ 3 in rectangular prism.

The aircraft's components and its controller must fit in to a carrying case that has interior dimensions of 20 in $\times$ 20 in $\times$ 20 in. Two people must be able to take the aircraft from its carrying case and fully assemble it in under 3 minutes. The aircraft is considered "fully assembled" when the radio controller is used to actuate the control surfaces of the aircraft.

The aircraft must be able to takeoff within 100 ft, fly a circuit of the flying area, and land within a designated landing zone 200 ft long. During the flight, the aircraft must maintain controllability so as to not pass into the no-fly zones. The aircraft must remain intact throughout the flight and landing, with the exception of the propeller, which may be damaged upon landing.

The scoring system necessitates that, for a competitive score, the aircraft must be both as light as possible and carry as much weight as possible.

DESIGN OVERVIEW

DESIGN PLAN The first step in design of the aircraft was to select a configuration. The team chose a traditional monoplane, due to the simple nature of the analysis required to evaluate a monoplane design. It was decided that the wing should be on top of the fuselage, for roll stability. To maximize lifting area, the team determined that the main wing would disassemble in to two halves, each which would fit inside the carrying case. To construct an appropriately large fuselage that will also fit in the carrying case, the fuselage must also disassemble in to two parts, and the tail must detach from the fuselage.

An analysis of the structure factors of the fuselage, tail, and wing of last year's winning Micro Class competitor from the University of Minnesota gave the team a rough estimate of the weight per unit area and volume of the components of the type of aircraft we were building. Further examination of power loading and wing loading of comparable model aircraft allowed the team to optimize the design with respect to the flight score equation within the constraints of carrying case dimensions.

Figure 1: Complete aircraft structure design.

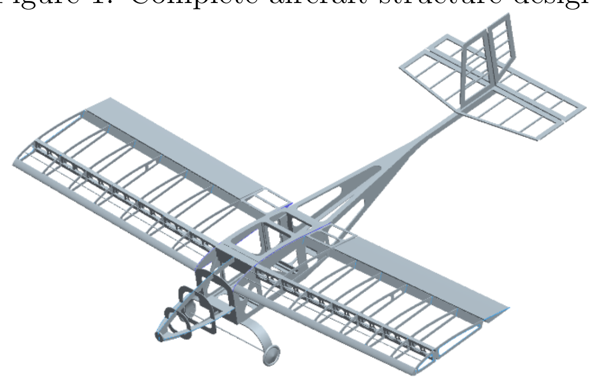

DESIGN EXPOSITION The driving parameters of this design were to engineer an aircraft of minimum empty weight, which can carry a significant payload fraction. Another goal was, whenever possible, to design the aircraft for ease of construction. In order to meet the design criteria of fitting in the carrying case, the aircraft had to be broken down into several parts. The wing is composed of two halves which connect to the fuselage. In addition, the fuselage separates at the point where the payload box connects with the beginning of the tail arm.

The electronics and propulsion components selected are comprised of the lightest commercially available products that the team was able to find that still effectively power the aircraft and actuate the control surfaces. The aircraft is powered by the Electrifly Rimfire 28-26-1600 electric motor along with a 9x4 propeller.

The fuselage is rectangular in shape. The main box of the fuselage has a height of 4.8 in, a width of 4.75 in, and a length of 11 in. The nose section of the fuselage is 7 in long, and the tail moment arm is 28 in. The nose and tail sections provide smooth aerodynamic transitions on the fuselage to minimize drag.

The wing disassembles in to two halves for storage in the carrying case mandated by the rules. It has a rectangular plan form, for ease of construction and maximum lifting area. The wing uses an S7055 airfoil section, chosen for both sufficient lift capabilities and manufacturability. The internal structure features a main spar at the aerodynamic center of the wing, with perpendicular ribs that define the shape of the wing. The wing has flaperons, control surfaces that act both as lift-increasing flaps and ailerons that control the roll rate of the aircraft.

The tail features a conventional design, with the horizontal stabilizer at the base of the vertical stabilizer. Both the horizontal and vertical stabilizer have a flat plate cross-section to minimize weight and facilitate construction. Both portions of the tail have control surfaces on their entire trailing edges, serving as the elevator and rudder of the aircraft. The aircraft is expected to have an empty weight of no more than 21 oz, and will carry a payload of up to 74 oz, for a maximum payload fraction of 0.76. When carrying its maximum payload, the aircraft will cruise at approximately 25 MPH.

Table 1: Design parameters of the wing and tail

	Main Wing	Horiz. Tail	Vert. Tail
Cross-Section	S7055	Flat	Flat
Span Length	50.0 in	17.4 in	6.3 in
Root Chord	12.0 in	7.3 in	6.95 in
Aspect Ratio	4.21	2.66	1.03
Taper Ratio	1.0	0.8	0.75
Sweep Angle	0°	9.75°	12.4°
% Control Surf.	21%	40%	40%

LEVEL-ZERO SIZING The starting point of sizing the aircraft was first to understand the flight score equations. The flight score FS for a flight is given by [1]:

$$FS = (10 - EW) \times PF \times 13 \quad (1)$$
$$PF = \frac{EW}{EW + PW} \quad (2)$$

where EW is the aircraft's empty weight, in pounds; and PW is the weight of the carried payload, in pounds. Thus, the total flight score is a function of the empty weight of the aircraft and the payload carried by it, as shown in Figure (2).

Figure 2: Flight score plotted against empty weight and payload weight.

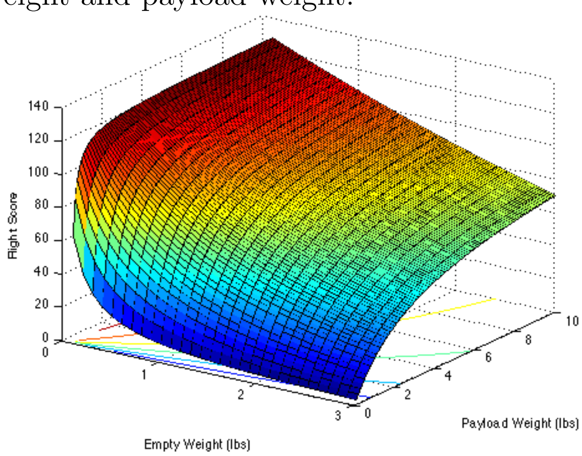

The first step in sizing the aircraft was to examine existing radio controlled aircraft to determine acceptable specifications for wing loading and power loading. Higher wing loading was determined to be desirable, as it results in less empty weight per unit of payload lifted. Similarly, minimizing power loading results in a lower empty weight due to smaller electronics. Based on information found in Lennon[4] for aircraft of similar size, the team chose a wing loading of 25 oz/in^2 and power loading no lower than 35 W/lb.

The second step was to examine the Micro Class aircraft that the University of Minnesota built last year. By disassembling it and weighing the components, the team was able to determine a formula for the weights of the wing and tail based on their plan form area, and the fuselage based on its length.

Next, an Excel spreadsheet was created that, given a wing size and desired wing loading, would calculate an empty weight for the structure of the aircraft and maximum takeoff weight. Using the resulting takeoff weight, the team chose a motor and associated electronic systems in order to achieve the desired power loading specification. Adding the weight of the electronics to the weight of the structure resulted in the design empty weight of the aircraft.

Once the electronics were specified for a design, the wing area and the other parameters that follow were varied to maximize the flight score of the aircraft. If needed, the electronics were re-specified, and the process was re-

Figure 3: Flight score plotted against payload weight. Each dark curve represents a different empty weight, indicated at the top of the plot. The black dot indicates the location of the designed aircraft.

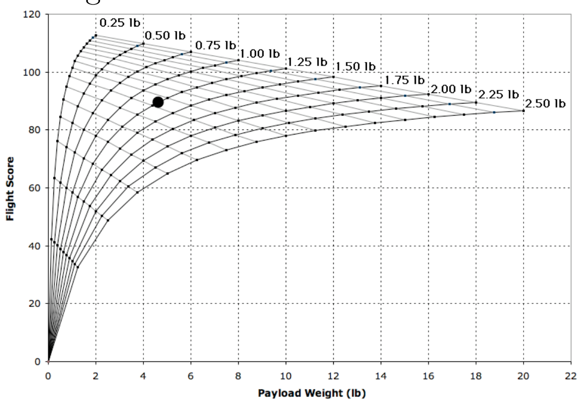

peated. After several iterations, the process converged to a conceptual aircraft with a wing area $S_W = 543$ in^2, chord $c_W = 12$ in, a target empty weight of 20 oz, and a maximum payload of 74 oz, leading to a payload fraction of 0.76, and a flight score of 89.6. Figure (3) shows the designed aircraft's location on the scoring curve.

WING DESIGN

The size of the wing was a major constraining factor in the level-zero sizing of the aircraft; the Micro Class carrying case allows for a maximum wing length of about 28 in with a 12 in chord, by placing the wing across the longest diagonal of the carrying case. By designing the wing to disassemble in to two parts, the team was able to achieve a 50 in span, resulting in 543 in^2 of lifting area.

Figure 4: Wing Structure Design.

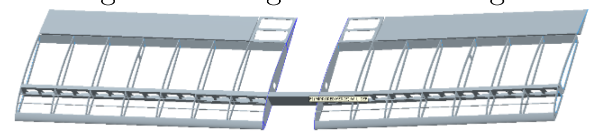

SHAPE AND SIZE The wing was chosen to have a rectangular plan form to maximize the lifting area. No taper, sweep, or twist were included, because the team decided that the aerodynamic benefits of these features was outweighed by those of simplifying construction. 3° of dihedral were added for enhanced lateral stability.

AIRFOIL SELECTION The airfoil shape was kept simple for ease of construction and strength. Because the overall design of the aircraft is very lightweight, it was determined that an extremely high lift airfoil featuring high camber and a thin trailing edge was not necessary; the S7055 flat-bottomed airfoil supplies adequate lift, while being thick enough to contain a sturdy internal structure, and has no inward camber or thin trailing edges that would make construction and skin application difficult.

Figure 5: S7055 Airfoil, used as the cross-section of the main wing.

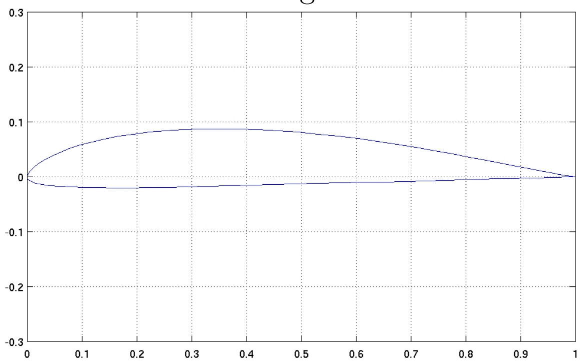

PERFORMANCE SPECIFICATIONS According to level-zero sizing, the wings are required to lift 5.89 lb. The lift curve data for the S7055 Airfoil [6] at an angle of attack $\alpha = 4°$ gives $C_L = 0.79$. Therefore, according to

$$L = 1/2 \rho V^2 C_L S, \tag{3}$$

the wing will be capable of lifting 7.13 lb at the cruising speed of 25 MPH determined by level-zero sizing, resulting in a safety factor of 1.22 with full payload.

WING STRUCTURE The wing will be constructed using a traditional spar-rib layout: a primary spar across the span of the wing acts as an anchor for all of the components of the wing and transmits the wing loads to the fuselage. Attached to the wing are chord-wise ribs that define the airfoil shape of the wing, and transmit the aerodynamic loads to the spar. The spar is at the aerodynamic center of the wing (the quarter chord), where there is zero net torque on the spar, reducing the torsional load on the spar, which in turn reduces its weight. The quarter chord is also near the point of maximum thickness of the S7055 airfoil, allowing for a large spar to be built within the wing.

Several concept test spars were designed and built to determine the best spar configuration. Spars tested included an I-beam, a C-channel, a two-part spar, and a box beam. Each spar was put through an identical three-point bending test to determine its flexural and ultimate strength. Through this test, the best design for the wing spar was determined to be a box beam, formed by adding webbing to a two-part spar: A larger balsa spar is on the top and bottom surfaces of the wing, joined by webbing for additional strength. Holes were cut in the webbing for weight savings.

The wing structure will be covered in lightweight Monokote film to provide a smooth aerodynamic surface on the wing. This has the added effect of tying together all the internal structural components and completing a torque tube, giving the wing additional

Figure 6: Detail of the wing spar, showing the box beam and holes in the webbing.

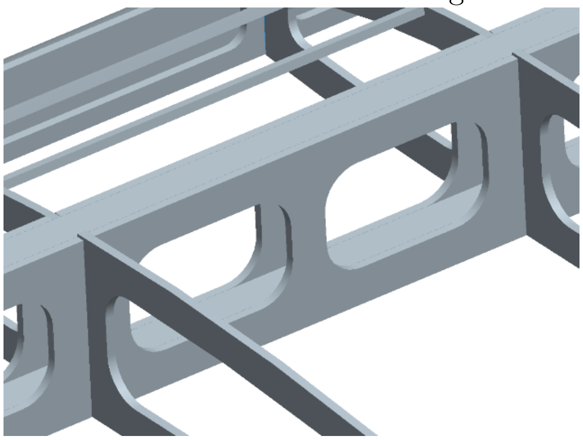

strength in all degrees of freedom.

WING ATTACHMENT The two halves of the wing will be attached to not only the fuselage, but also each other to ensure that the fuselage does not have to carry a large bending load due to the cantilevered nature of the wing. This is achieved by manufacturing the left and right spars such that, at the root, each half of the wing composes one half of the box beam structure. Then, these two halves are bolted together to form one continuous wing. The same bolts used to attach the wing halves to each other also fasten it to the fuselage.

Full-scale prototypes of the wing and fuselage were built and tested. The wing attachment mechanism held over 50 lb without failing, giving a safety factor of 2.8 in a 3g loading scenario.

FUSELAGE DESIGN

FUSELAGE DESIGN The design constraint with the most impact on the fuselage design was the payload box dimensions of 8 in × 4 in × 3 in. To accommodate this, the fuselage was designed to be rectangular, with the long axis of the box down the center line of the aircraft. The payload box was oriented with the 4 in dimension horizontally to minimize the height of the fuselage and give a wider area above the box to attach the wings.

Figure 7: The fuselage structure design.

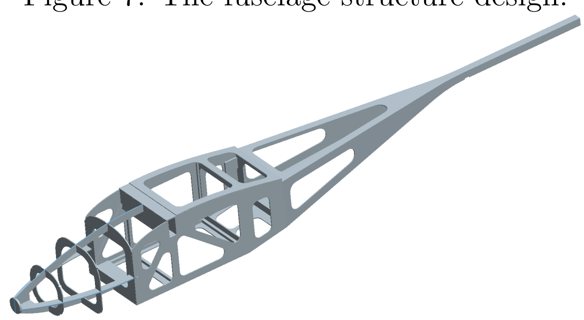

The nose and tail fairing sections were designed using standard aerodynamic rules of thumb. The nose is about 1.5 times the maximum width of the fuselage, and the tail fairing section is about 3.5 times the maximum width of the fuselage, to ensure that there is no flow separation around the fuselage, so that minimum drag is achieved.

FUSELAGE CONSTRUCTION After considering carbon fiber and other materials for the fuselage, balsa wood was determined to be the best material for the majority of the structure. According to the team's analysis, the extra strength of composites was not worth the additional weight. Most of the fuselage is made of 1/16 in balsa sheet with 1/8 in or 3/16 in balsa stick glued in corners for reinforcements. The nose of the plane is constructed with 1/16 in plywood to ensure it can adequately transmit the loads of the motor to the fuselage. The wing attachment and joint between fuselage sections are built with 1/8 in plywood for strength, since it is critical that these components do not fail. The parts were cut on a laser cutter for accuracy and glued together with cyanoacrylate adhesive.

TAIL DESIGN

The tail features a conventional design, with the horizontal stabilizer at the base of the vertical stabilizer. Both the horizontal and vertical stabilizer have a flat plate cross-section to minimize weight and facilitate construction. Both portions of the tail have control surfaces on their entire trailing edges, serving as the elevator and rudder of the aircraft.

Figure 8: Tail structure design.

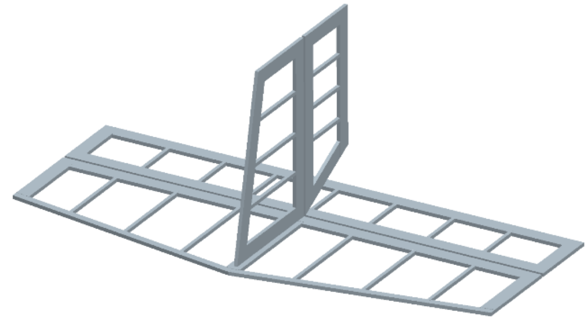

HORIZONTAL STABILIZER The area S_{HT} of the horizontal tail was calculated by

$$S_{HT} = C_{HT} \frac{c_w S_w}{l_{HT}} = 116 \text{ in}^2 \tag{4}$$

where the horizontal tail volume coefficient $C_{HT} = 0.5$. This value is slightly smaller than the minimum recommended in Lennon[4], but it was shown to be adequate in last year's top-scoring University of Minnesota Micro Class entry.

VERTICAL STABILIZER The area S_{VT} of the vertical tail was calculated by

$$S_{VT} = C_{VT} \frac{c_w S_w}{l_{VT}} = 38 \text{ in}^2 \tag{5}$$

where the vertical tail volume coefficient $C_{VT} = 0.04$. Similar to the sizing of the horizontal stabilizer, this value is slightly smaller than the minimum recommended in Lennon[4], but it was again shown to be adequate in last year's entry.

CONTROL SURFACES

FLAPERONS Flaperons are used in the design primarily to give the aircraft roll control. In addition, they double as flaps, for added lifting capability during takeoff and acting as air brakes when landing. The flaperons span 85% of each wing's semi-span to achieve a large amount of roll authority and extra lift when needed. 25% of the wing's chord length, as recommended by Lennon[4].

Flaperons were chosen over the more traditional set up where there are two ailerons and two flaps because of the savings in weight, as less control linkages and servos are required. Other considerations included the cost savings by not having to purchase more electronics, easier first flights with less control surfaces, and overall simpler construction.

ELEVATOR From Corke [3], the elevator area is nominally 40% of the horizontal stabilizer:

$$S_{Elev} = 0.4 \times S_{HT} = 46.4 \text{ in}^2 \qquad (6)$$

RUDDER From Corke [3], the rudder area is nominally 40% of the horizontal stabilizer:

$$S_{Rudd} = 0.4 \times S_{VT} = 15.2 \text{ in}^2 \qquad (7)$$

CONTROL SURFACE CONSTRUCTION The flaperons will be constructed from foam in order to preserve the integrity of the airfoil's shape, while the rudder and elevator will be constructed from a balsa wood framed flat plate covered in Monokote. Four servos will be used to actuate the control surfaces: one for each flaperon, one for the rudder, and one for the elevator. Piano wire control rods will connect the servos to control horns on each control surface.

A medical tape called "Blenderm" will be used to hinge the control surfaces. Tape provides many advantages over a conventional hinge: it is lightweight, easy to install, and it has been shown to provide a damping effect to prevent control surface flutter.

LANDING GEAR

The "tail dragger" landing gear configuration was chosen for the aircraft over a conventional three-wheel layout because of its light weight and simplicity. The rear "dragging" wheel does not have to be very strong, thus effectively limiting the structure of the system to the main landing gear. In addition, because the rear wheel is in the back, only a simple linkage is needed between the rudder and rear wheel for steering control, instead of a separate linkage to the front of the aircraft. This configuration also has the added benefit of increasing the aircraft's angle of attack on takeoff.

The main landing gear for the aircraft must be strong enough to withstand a 3g load from the combined airframe and payload, equal to 18 lb. It must also be rigid enough to prevent excessive deflection (determined to be 0.5 in) at the maximum 3g loading and at the same time be as light as possible. Landing gear from similarly sized model aircraft lead the team to select a 10 in span between the wheel struts. The size of the propeller required the height of the gear to be no less than 3 in. The placement of the landing gear was dictated by where the strongest connection could be made to the fuselage, and far enough forward of the center of gravity to keep 10-15% of the weight on the rear wheel.

Figure 9: The landing gear design.

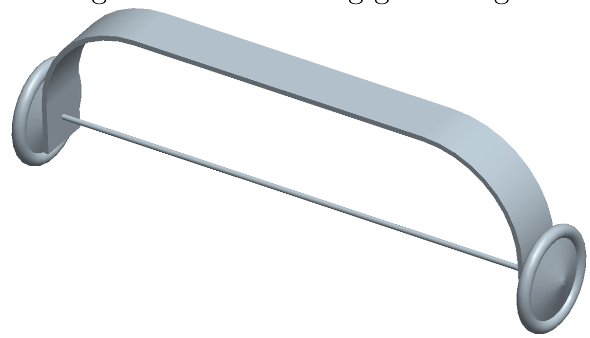

The team determined that all the commercially available gear in the desired size and strength were too heavy for this application. Based on previous experience with composites, the team felt confident that it was possible to construct custom carbon fiber landing gear that would weigh less than commercially available solutions. Three prototypes were constructed, varying the number of layers of fabric as a test parameter. These prototypes were then loaded statically as shown in Figure (10).

Figure 10: Static testing apparatus used to determine landing gear strength.

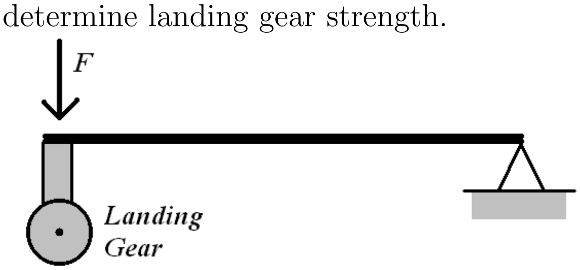

The results of the test are listed in Table 2.

From these tests, it was determined that the extra strength and safety factor of the 7 layers

Table 2: Landing gear prototype static loading test results.

Fabric Layers	Weight	Load at Failure
4	31.5 g	19 lb
5	35.5 g	24 lb
7	36.5 g	30 lb

of fabric was worth the extra 5 g of material over the 4- and 5-layer models. Lightweight plastic wheels were attached to the composite struts with a solid wire axle between the two wheels.

PROPULSION

The propulsion system must be powerful enough for the aircraft to take off in less than 100 ft, and must do this when carrying even its maximum possible payload. Other factors considered were commercial availability, reliability, and ease of use.

A study was done comparing the use of an electric motor and a gas engine. Due to the scale of the aircraft, it was decided that an electric motor would be better suited to the requirements: electric motors can supply ample thrust while remaining lightweight and are also gentler on the aircraft due to reduced vibration over gasoline engines. Electric motors have the added benefit of being significantly easier to use and maintain.

After the decision to use an electric motor was made, a more in-depth study was conducted to determine the motor and battery combination that would result in the highest flight score. To aid in this decision, a MATLAB program was developed that analyzed the theoretical power output for different motors, battery, and propeller combinations based on the motor and battery's electrical properties. This analysis narrowed the selection to two motors: the Purple Peril from Little Screamers, and the Rimfire 28-26-1600 from Electrifly. These motors were then compared with two different Lithium Polymer batteries from Thunderpower, a 730 mAh, 11.1 V battery pack and a larger 910 mAh, 11.1 V pack. While the 730 mAh pack is lighter, the 910 mAh pack has a greater current limit and can therefore provide more power.

Analysis of the takeoff roll and the scoring equation showed that, although the Rimfire is heavier than the Purple Peril, when combined with the 910 mAh battery, it yields a higher potential flight score.

Therefore, the choice was made to use the Rimfire 28-26-1600 in conjunction with the

Thunderpower 910 mAh, 11.1 V LiPo battery.

The same MATLAB simulation of the motor was also used to determine the optimal propeller for this motor-battery combination. Results can be seen in Figure (11). Using these

Figure 11: Theoretical Thrust vs. Speed for Rimfire 28-26-1600 motor and ThunderPower 910 mAh, 11.1 V LiPo battery pack using 9 in diameter propeller at various pitches.

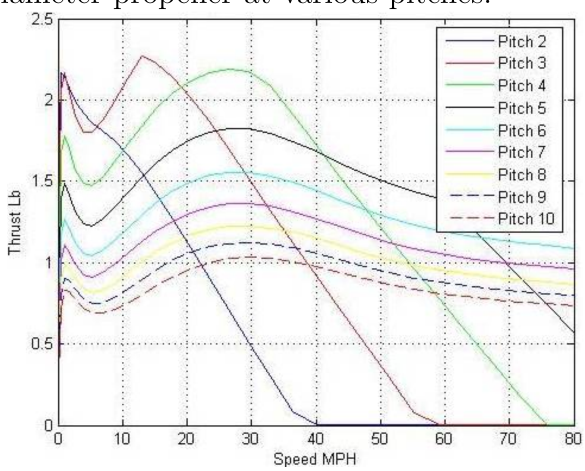

results and the predicted speed required for level flight (known from Level-Zero Sizing), it was concluded that a 9x4 propeller was the best for this aircraft, as it would give sufficient thrust for all foreseeable speeds of the aircraft.

ELECTRONICS

After choosing the motor and propulsion battery, the rest of the electronics were chosen to fit with this configuration while minimizing weight and maximizing reliability. The other components include a 20 A Hacker X-20-PRO speed controller, a Futaba RG17FS 2.4 GHz spread-spectrum radio receiver, a 4.8 V NiMH battery pack to power the receiver, two Scanner RC Ball Bearing servos to actuate the flaperons, and two Blue Arrow Micro servos to actuate the elevator and rudder.

A diagram of the wiring of the electronics is in Appendix A.

PERFORMANCE ANALYSIS

Lift is of course the primary concern of a competitive heavy-lift aircraft. However, of secondary concern, but still essential, is an aircraft's ability to perform its intended function well. The aircraft must have low enough drag (or high enough power) to produce the forward velocity to provide the required lift and take off within a prescribed distance. In addition, the aircraft must be dynamically stable while in the air, which is mostly a function of the location of critical aerodynamic components relative the center of gravity.

DRAG ANALYSIS A drag analysis, shown in Figure (12), was performed based on Dr. Leland M. Nicolai's White Paper on estimating the performance of R/C aircraft

[5]. It was assumed that the drag due to

Figure 12: Drag polar curve generated from Nicolai's method of drag analysis.

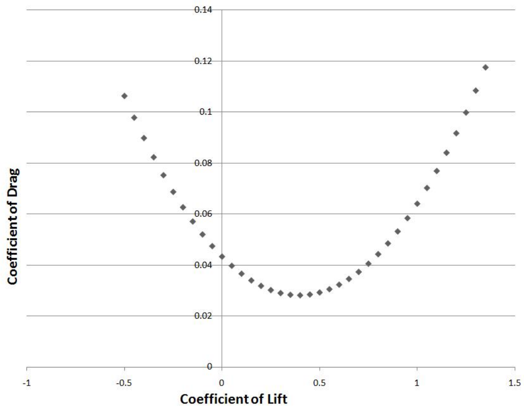

the landing gear and the engine would be negligible compared to other components, and thus those components were left out of the calculation. For the aircraft, using Nicolai's method [5]:

$$C_{D_{min}} = 0.022 \tag{8}$$

Professor Jeff Hammer, a University of Minnesota instructor, supplied his own drag analysis spreadsheet, which he had previously developed, to the team. The spreadsheet predicted that $C_{D_{min}} = 0.023$, which is in agreement with Nicolai's method. The value for $C_{D_{min}}$ is useful in creating a drag polar curve, and providing a good drag estimate for takeoff roll approximations. Wind tunnel data for the S7055 airfoil obtained from the University of Illinois at Urbana-Champaign [6] was used to complete these calculations.

3D DRAG EFFECTS Wingtip vortices occur on any finite wing when it produces lift. The effect of this is an induced downwash across the wing cross-section, which reduces lift and increases drag. The team considered using winglets or other vortex-reducing devices on the wingtips, but it was determined that adding such a device would increase the size of the wing enough that it would not fit in to the aircraft's carrying case. In addition, the specified motor has enough excess power to overcome the drag due to wingtip vortices.

TAKEOFF ANALYSIS Rule 20.1.2 for the SAE Aero Design competition states that "Micro Class aircraft must lift from the ground within a takeoff zone measuring 100 feet in length." Again, using Dr. Leland M. Nicolai's White Paper [5], a takeoff roll approximation was made using the results from the drag analysis and airfoil data on the S7055 from the University of Illinois at Urbana-Champaign, shown in Figure (13). Like Nicolai's analysis, this is a conservative one, assuming that the aircraft will be taking off in atmospheric

Figure 13: Takeoff Distance vs. Payload. The circular markers denote values from Professor Hammer's code, while the diamond-shaped markers denote values from the code that used Dr. Nicolai's method. The colors blue, red, and green refer to maximum coefficient of lift values of 1.1, 1.3, and 1.5, respectively.

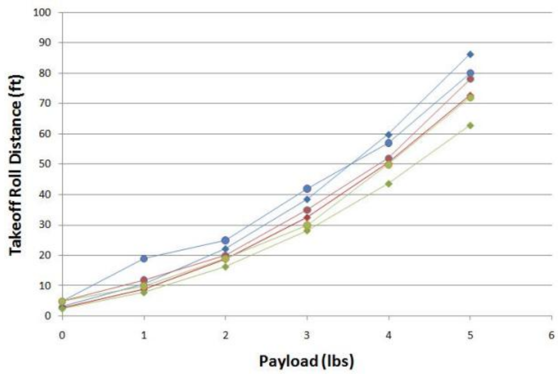

conditions at 3000 ft above sea level, and only using 80% of the available power.

In this simulation, the empty weight of the aircraft was assumed to be 1.28 lb. The payload and lift values were varied to simulate different loading conditions and flap settings. Again, Professor Jeff Hammer provided a good comparison tool, this time in the form of a MATLAB/Simulink code which simulated the takeoff of an aircraft. The results from both methods agreed, thus confirming the results.

STABILITY ANALYSIS In order to successfully fly, the aircraft designed must have static stability. A longitudinal controls-fixed stability is achieved when [2]:

$$\frac{dC_m}{dC_{LW}} = (h - h_0) - \eta V_T \left(\frac{a_1}{a} \left(1 - \frac{d\epsilon}{d\alpha} \right) \right) < 0 \quad (9)$$

where $h = 0.25$ is the location of the center of gravity from the leading edge of the wing, $h_0 = 0.25$ is the location of the aerodynamic center of the wing, $\eta = 0.6$ is the stabilizer efficiency for a conventional tail [7], V_T is the tail volume coefficient. $a_1 = 3.12$ rad^{-1} is the lift curve slope of the horizontal tail, $a = 4.12$ rad^{-1} is the lift curve slope of the wing. Both lift curve slopes were calculated using thin airfoil theory and correcting for finite wing effects using the aspect ratio AR [5]:

$$a = \frac{2\pi AR}{2 + (4 + AR^2)^{1/2}} \quad (10)$$

$\frac{d\epsilon}{d\alpha}$ is the change stabilizer downwash angle versus the change in wing angle of attack. Typical values for the change in stabilizer downwash angle versus the change in the wing angle of attack are between 0.33 to 0.5, so a value of 0.4 was used [7].

Using Equation (9), the stability margin K_n for this aircraft is

$$K_n = -\frac{dC_m}{dC_{LW}} \times 100\% = 14\% \quad (11)$$

The neutral point is another useful parameter, as it provides a good reference point for locating the center of gravity. The neutral point is defined as the point where all of the aerodynamic forces are in equilibrium with each other. The neutral point h_n is calculated by [2]

$$h_n = h_0 - \eta V_T \left(\frac{a_1}{a} \left(1 - \frac{d\epsilon}{d\alpha} \right) \right) = 0.39 \quad (12)$$

It is important to note that when the aircraft is empty, it is unstable. Only when carrying a payload, strategically placed in the payload box, is stability achieved. This is not a concern, as the predicted payloads are much heavier that the predicted empty weight of the aircraft, thus making it easy to shift the aircraft's center of gravity. The minimum load that the aircraft can carry while maintaining stability is 29 oz, located at the front limit of the payload box.

FUSELAGE STRUCTURAL ANALYSIS
After the selection of the fuselage design, a finite element analysis was performed on the computer model using the ANSYS 11.0 software package. The objective of this was to estimate the location and magnitudes of the stress concentrations as well as the resulting deflections. Assumptions were made of the non-isentropic balsa wood to approximate isentropic behavior. This included the assumption that the loading would occur against the grain of the wood to maximize the strength of the material. This is a good assumption because the airframe will be constructed with this as a guiding principle. The properties were then generalized according to the properties specified by the retailer Tower Hobbies. The balsa used had a specified density of 10 oz/ft^3, with compressive strength of 1890 psi and tensile strength of 1910 psi.

The applied loads were: 4.8 lb distributed load on the payload box, 6.0 lb distributed load across the wing spar support box, two 3.0 lb point loads at the landing gear and a 0.5 lb load distributed across the last 5 in of the tail spar. All of these loads were multiplied by a safety factor of 3.

The resulting simulation created several points of interest. As discussed previously, the fuselage is collapsible into two pieces about the center. The connection points created a local maximum stress of 1336 psi. The resulting deflection of the tail under a triple loading was only about 0.25 in, resulting in an angle of attack adjustment of 2.8°. The last area of interest occurred about the two points of contact for the landing gear which created local stress concentration of 1913 psi. These results were integral in the design of the fuselage failure test as well as highlighting areas to reduce structurally to save weight.

Figure 14: Finite Element Analysis of the fuselage. Analysis was performed on only half of the fuselage due to symmetry. A stress concentration of 1913 psi was found at the landing gear contact points.

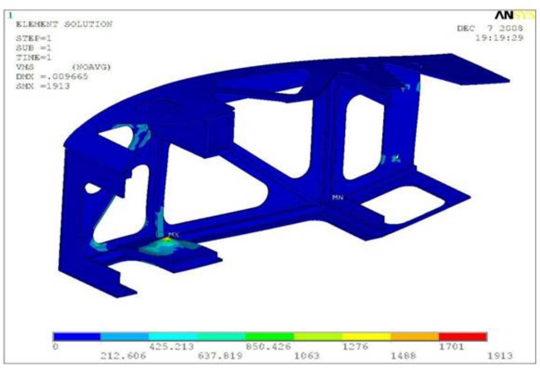

Figure 15: Finite Element analysis of the tail section of the fuselage. Max deflection at the tail is 0.25 in from a 3 lb distributed load on the tail area.

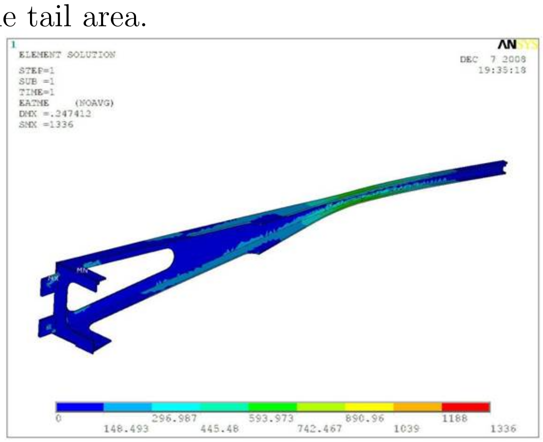

PROTOTYPE BUILDS

Before this project, the team collectively had very little experience with building remote control aircraft. Therefore, building a preliminary prototype of our design not only remedied this situation, but allowed for verification of design manufacturability and strength. During the build, we were able to identify several areas of improvement in the team's design. There were several areas in the wings that needed re-enforcement, and several areas in the fuselage that could be lightened up from the original design. To quantify these observations, the wings, fuselage and landing gear were statically loaded to determine points of failure. These revisions were added to the model and will be incorporated in the next version of the aircraft, which will be built to fly.

Figure 16: Prototype build of the aircraft design, without the tail.

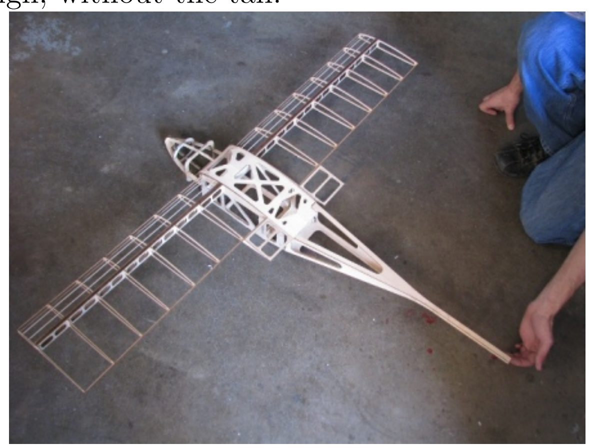

CONCLUSION

Designing and building a Micro Class aircraft was both challenging and exciting. The team's goals of minimizing weight and ensuring ease of construction, our effort to fully understand the scoring equation, and knowledge of previous successful designs allowed us to justify our design decisions in a timely manner. The knowledge gained from last year's University of Minnesota team was of key importance in that it provided a baseline for work done this year.

REFERENCES

[1] 2009 SAE Aero Competition Rules Document

[2] Cook, Michael V. *Flight Dynamics Principles*, 2nd Edition. Butterworth-Heinemann, Burlington, MA, 2007.

[3] Corke, Thomas. *Design of Aircraft*. Pearson Education, Upper Saddle River, NJ, 2003.

[4] Lennon, Andy. *Basics of R/C Model Aircraft Design*. Air Age, Wilton, CT, 1996.

[5] Nicolai, Leland M. *Estimating R/C Model Aerodynamics and Performance*. Lockheed-Martin, 2002.

[6] Selig, Michael, *UIUC Airfoil Data Site*, University of Illinois at Urbana-Champaign (Illinois), http://www.ae.uiuc.edu/m-selig/ads.html, 2008.

[7] Simon, Martin. *Model Aircraft Aerodynamics*, 4th Edition. Trans-Atlantic Publications, 1999.

ACKNOWLEDGMENTS

- Prof. Jeff Hammer, University of Minnesota
- Greg Nelson, University of Minnesota
- Chris Launer, Lockheed-Martin
- MARCEE
- Hub Hobby Center
- The University of Minnesota
- University of Minnesota Solar Vehicle Project
- Parametric Technology Corporation (PTC)
- The LaTeX Project

APPENDIX A: WIRING LAYOUT